# COMPARATIVE STUDY ON PROTECTIVE PERFORMANCE AND MATERIAL OPTIMIZATION OF AUTOMOBILE BUMPERS UNDER DIFFERENT COLLISION CONDITIONS

Yanling ZHAO[1], Kai KANG[2, *], Jiaqing ZHANG[3], Junchao LI[2]

*Improving the collision safety of automotive bumpers under low-speed conditions is a crucial research topic in vehicle safety. This paper studies the collision energy absorption characteristics of bumpers under three working conditions, namely 100% frontal collision, offset collision and 60° angled collision. Meanwhile, the thickness and material of the bumpers are replaced. The research results show that both the optimized and pre-optimized bumper structures can meet the requirements of the national standard GB/T 17354-2024, but there are certain differences in the collision results. Therefore, when studying the collision safety of bumpers, considering both material and structural thickness is an important factor to improve the performance of bumpers.*

**Keywords**: Bumper; Energy Absorption Characteristics; Low-Speed Collision; Thickness Optimization; Material Optimization

## 1. Introduction

As an indispensable means of transportation in people's daily lives, the development of automotive safety technology has attracted significant attention, particularly in terms of safety performance. According to incomplete statistics, low-speed collisions account for approximately 55% of all automotive collision accidents [1]. This is mainly because when a collision is imminent, drivers will rapidly reduce the vehicle's speed to minimize losses, resulting in low speeds under most collision conditions. Although the speed of vehicles involved in low-speed collision accidents is relatively low, such accidents can still cause vehicle damage, pedestrian injuries, and economic losses. The primary cause of losses from such accidents lies in the improper selection of materials and structures for the crossbeams and energy absorbers. This improper selection leads to severe deformation when two vehicles collide, which in turn crushes other automotive components and triggers a chain reaction. Consequently, countries worldwide have established clear regulations on vehicle low-speed collision performance in

1 * Corresponding author, Zhangjiakou LUYUAN Highway Engineering Co., Ltd. E-mail: 18713356856@163.com
2.School of Mechanical Engineering, Hebei University of Architecture
3. Department of Energy Engineering, Hebei University of Architecture

their automotive safety standards. For instance, China has GB 17354 (*Requirements for Front and Rear End Protective Devices of Motor Vehicles*) [2], the European Union has ECE R42 (*Uniform Provisions Concerning the Approval of Vehicles with Regard to their Protection in the Event of a Low-Speed Collision*), and the United States has FMVSS Part 581 (*Bumper Safety Standards*). These regulations require that automotive bumpers effectively absorb impact forces during low-speed collisions to reduce vehicle damage and personal injuries. Therefore, researching the energy absorption effect of automotive bumpers and energy-absorbing devices under low-speed collisions holds significant value for ensuring the safety of passengers and drivers.

In the early stage of enterprise technology development, bumper performance testing relied on real-vehicle collision tests to obtain relevant data. However, this method not only incurs high costs and requires a long time but also makes the collection and comprehensive analysis of experimental data difficult. In contrast, the finite element analysis software LS-DYNA is much simpler and more accurate. Using this software, researchers can accurately simulate the deformation mode, stress distribution, and energy absorption of automotive bumpers during low-speed collisions in a virtual environment [3]. This enables the acquisition of accurate experimental data, allowing researchers to better analyse and understand the energy absorption characteristics of bumpers. As a result, a large amount of human and material resources are saved, while the accuracy of experimental data is ensured.

In recent years, scholars have achieved numerous research results in the field of automotive bumper performance research.

In terms of material improvement, Li et al. [4] proposed a new theory regarding high-carbon-induced embrittlement at the interface between aluminum-silicon coatings and steel substrates, and developed an interface carbon reduction and toughening technology. The application of this technology can improve the collision performance of components by 28% and significantly reduce the risk of cracking. Yu et al. [5] conducted extensive research on the vibration resistance of automobile frames filled with aluminum foam, confirming the feasibility of applying aluminum foam laminated structures to automobile bumpers; the use of this structure can significantly enhance energy absorption characteristics. The technical team of Yanfeng Visteon has focused on the integrated design of exterior parts and the application of lightweight materials. Through unremitting efforts, they have developed an injection molding process for bumper outer panels based on modified polypropylene (PP). By adding elastomers to the outer panels, the impact resistance under low-temperature conditions is improved, which can meet the collision safety performance requirements in environments as low as -30°C. The R&D team of Moulding Technology has developed carbon fiber-reinforced plastic (CFRP) bumpers. Compared with traditional materials, this type of material reduces weight by 40% and improves energy absorption efficiency by 25%, placing such bumpers at a world-leading level.

Meanwhile, enterprises and universities have also conducted extensive experiments on the material research of bumpers. Shim et al. [6] studied reusable energy dissipation devices and designed an energy-absorbing device composed of a cylinder and a flange. Through a hinge structure, the impact force is converted into the kinetic energy of the separation column, solving the problem that traditional energy-absorbing structures are damaged after collision. The collaborative team of Honda Motor and SABIC focused on the replacement of thermoplastic materials. Ultimately, they verified that replacing traditional expanded polypropylene (EPP) foam with an injection-molded thermoplastic (PC/PBT) energy absorber can enable the material to have higher compressive strength in a smaller space, while reducing costs and weight. The aforementioned studies indicate that improving the material design of automotive bumpers is an important approach to enhancing the safety performance of bumpers at present.

In terms of structural design, Baykasoğlu et al. [7] conducted a study on optimizing and improving the performance of bumper structural anti-collision beams using a multi-objective optimization algorithm. Jin [8] adopted a multi-objective optimization model for bumper collision based on LS-DYNA, which significantly improved the accuracy of simulation predictions and achieved a technical breakthrough with an error of less than 5%. Wang et al. [9] used orthogonal experimental design to analyse the impact effect between bumpers and guardrails under different working conditions, pointing out that reasonable design of energy absorber and bumper wall thickness can improve the anti-collision performance of automobiles. Keval et al. [10] designed a bumper structure capable of reducing pedestrian casualties, and experiments proved that improving the bumper structure can reduce collision injuries to pedestrians. Gonçalves et al. [11] conducted a lightweight design of bus bumpers, compared the impacts of material optimization and structural improvement on the life cycle of buses, and pointed out that the structure of automotive bumpers should be reasonably designed to balance the economy and practicality of automobiles. Zhang et al. [12] improved the performance of road guardrails by adding rubber pads and energy-absorbing rings, indicating that improving the detailed design of anti-collision structures is of great significance for enhancing the safety performance of anti-collision energy-absorbing devices.

In summary, existing research on automotive bumper performance has achieved remarkable progress in both material innovation and structural design. In terms of materials, scholars and enterprises have developed interface toughening technologies for coated steels, verified the feasibility of foam aluminum laminated structures, and promoted the application of lightweight and high-energy-absorption materials such as modified PP, CFRP, and PC/PBT composites. In terms of structure, orthogonal experimental design and detailed structural improvement have been widely adopted to enhance crashworthiness. While pedestrian protection and lifecycle economy have been incorporated into structural design considerations. Collectively, these studies confirm that synergistic improvements in material selection and structural optimization are the core paths to enhancing the protective performance, lightweight level, and comprehensive applicability of automotive bumpers under low-speed collision conditions.

## 2. Finite Element Modelling of Automotive Bumpers

### 2.1 3D Modelling of Automotive Bumpers

Based on the design parameters of a specific automotive bumper and combined with the low-speed collision performance indicators specified in the national standard GB/T 17354-2024, this study investigates indicators of the bumper such as displacement, collision force, and acceleration. By modifying parameters of the bumper, including its structure and material, the protective performance of the bumper before and after modification is evaluated, thereby providing reasonable guidance for the improved design of the bumper.

First, according to the established 3D model of the bumper, the 3D model of the anti-collision beam is imported into Hypermesh software. Within the software, a finite element geometric model check is performed, and repair tools are used for preprocessing of its modelling structure. Finally, the bumper model is obtained as shown in Figure 1 below.

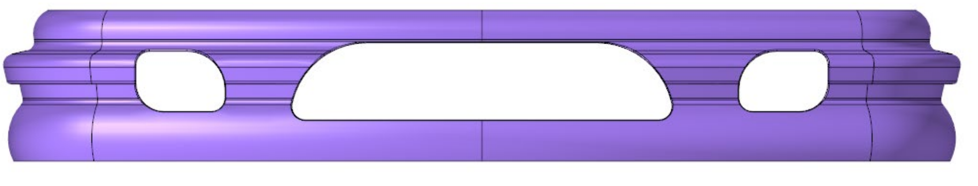

Fig. 1 3D Model of the Automotive Bumper

Finite element discretization was performed on this model, and the model is shown in Figure 2. During the discretization process, the mesh size of the original bumper was set to 5 mm, and the mesh size of the energy absorber was set to 4 mm.

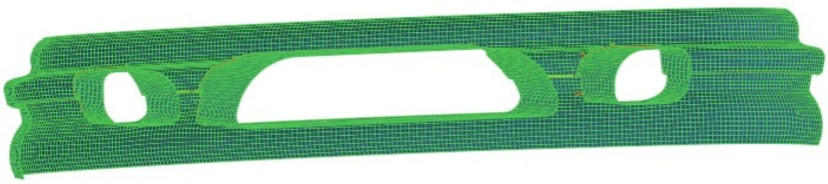

Fig. 2 Automotive Bumper Model After Discretization

The discretization quality assessment was conducted in HyperMesh, and the discretization evaluation results are shown in Figure 3.

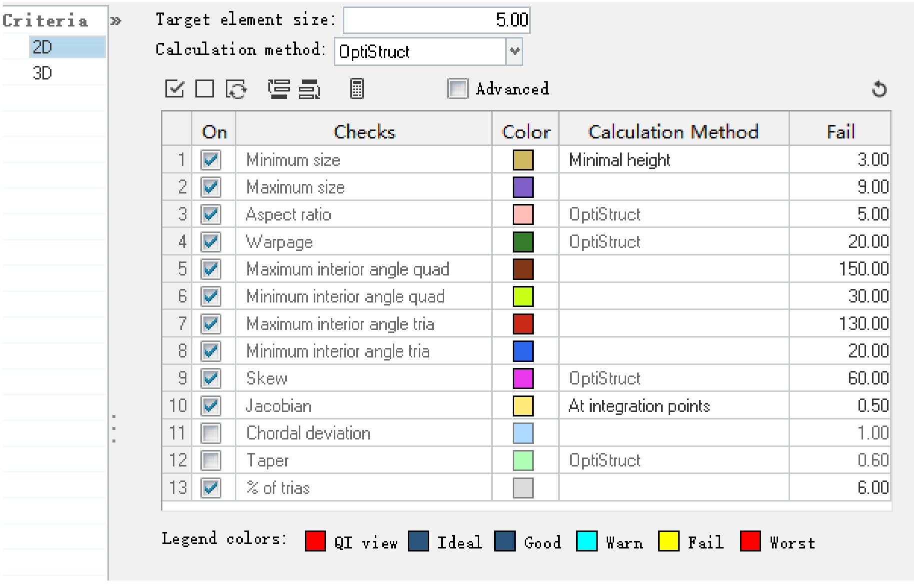


Figure 3 Discretization Quality Evaluation Results

Analysis shows that the bumper model has good discretization quality. 94% are qualified, and none of the evaluation indicators show the "Fail" status.

### 2.2 Setting of Collision Simulation Parameters

In the simulation, the impactor built into the software system is used for collision simulation with the bumper. Among them, the impactor is defined as a rigid body, and the bumper material is PP-LGF30 [13], which combines the mechanical properties of rigidity and plasticity. The material property parameters are shown in Table 1 below.

Table 1

**Material Parameters of PP-LGF30**

| *Material* | *Density (kg/m³)* | *Elastic modulus/ (GPa)* | *Poisson's ratio* | *Yield strength (MPa)* | *Thickness (mm)* |
|---|---|---|---|---|---|
| *PP-LGF30* | *1000* | *5600* | *0.37* | *39.1* | *3.5* |

To accurately describe the elastoplastic mechanical behavior of the bumper materials during low-speed collisions, the MAT_24 material card in LS-DYNA was used in the simulation. The elastic stage equation reflects the linear stress-strain relationship before yielding, the Von Mises yield criterion determines the initiation of plastic deformation, and the associated flow rule describes the development of plastic strain, ensuring the reliability of the simulation model.

### 2.3 Setup of Collision Simulation Working Conditions

During the collision process, the bumper is set as the active component, and the impactor is set as the fixed component. The dynamic friction coefficient is set to 0.15, and the static friction coefficient is set to 0.2. The collision effects of the automotive bumper under 100% frontal collision, offset collision, and 60° angled collision are studied respectively. The collision simulation model is shown in Figure 4, where the red part represents the automotive bumper and the green structure represents the impactor.

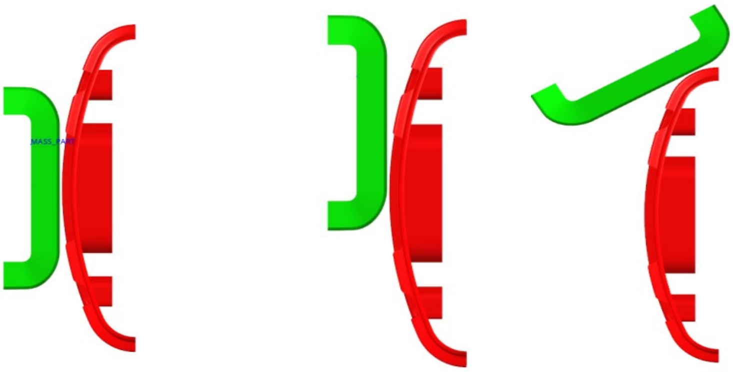

(a) Frontal Collision of Bumper (b) Offset Collision of Bumper (c) 60° Angled Collision of Bumper
Figure 4 Three Collision Modes

In this low-speed collision test, the impactor is set as a rigid body, and the actual vehicle mass (1000 kg) is assigned to it. In accordance with the national standard GB/T 17354-2024, the initial velocity of the impactor is 4 km/h in the frontal collision, and the numerical simulation calculation time is 0.1 s. During the collision process, the bottom of the model is fixed. In the frontal collision, the impactor can only move along the collision direction; therefore, remote displacement constraints are used to restrict all degrees of freedom except the collision direction [14, 15]. In the 60° angled collision, the plane of the impactor forms a 60° angle with the vertical direction of the bumper, the initial velocity of the impactor in the low-speed collision is 2.5 km/h, and the numerical simulation calculation time is 0.1 s.

## 3.Collision Result Analysis

### • *3.1* Rationality *Evaluation of Collision Simulation*

Figure 5 presents the curve of collision force versus time for the bumper during a 100% frontal collision. As can be seen from the figure, the collision force begins to appear at 0.007 s. Afterwards, as the impactor starts to contact the bumper and with the elapse of time, the collision force increases, which indicates that the impactor and the bumper gradually enter the collision process. At 0.04 s, the collision force of the bumper reaches a peak value of 56.1 kN. Subsequently, due to the complete consumption of the impactor's kinetic energy, the impactor gradually detaches from the bumper, leading to a gradual decrease in the collision force. By 0.075 s, the collision force drops to 0, which demonstrates that the impactor and the bumper have been completely separated at this moment and marks the end of the collision process. This process can well simulate the collision between the bumper and the impactor.

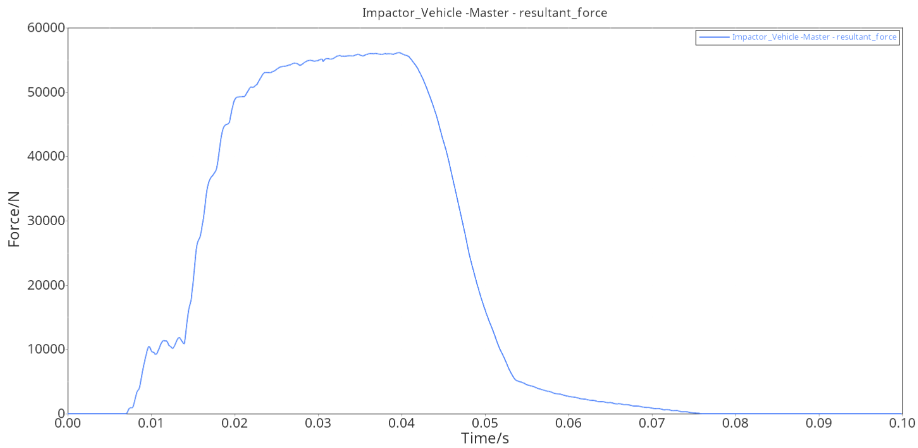


Fig. 5 Collision Force-Time Curve

Meanwhile, the hourglass energy in the 100% frontal collision was evaluated, as shown in Figure 6. The collision process is accompanied by energy conversion between the impactor and the bumper, and the curves of momentum, internal energy, hourglass energy, and total energy are presented in Figure 6. It can be observed from the figure that the total energy of the system is conserved, remaining constant at 735.21 J throughout the process. In the simulation model, the hourglass energy is 0.4 J, accounting for 0.1% of the bumper's internal energy. The proportion of hourglass energy in the system is far below 5%, which indicates that the model meets the requirements and the simulation results are accurate and reliable. During the collision, most of the impactor's kinetic energy is converted into the internal energy of the bumper, and this part of the kinetic energy is mainly absorbed by the deformation of the bumper structure.

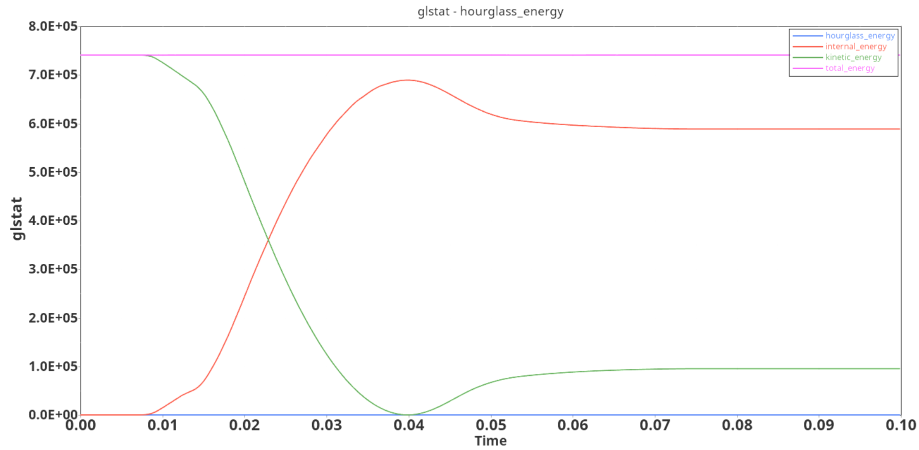

Fig. 6 Curves of Momentum, Internal Energy, Hourglass Energy, and Total Energy

From the above analysis, it can be concluded that during the collision process, energy leakage is almost zero, and the proportion of hourglass energy is very small, which is below the 5% threshold. Therefore, the parameters used to simulate the collision process between the bumper and the impactor are basically applicable. Meanwhile, it is also found that during the collision, the maximum impact force on the bumper is 56.1 kN, and the maximum energy absorption is 68.9 J.

### *3.2* **Analysis** *of 100% Frontal Collision Results*

The results of the 100% frontal offset collision were observed, as shown in Figure 7 below.


(a) t=10 ms (b) t=40 ms (c) t=90 ms

Fig. 7 Structural Deformation Diagrams of the Bumper at Selected Time Points

As analyzed from Figure 7, at the onset of the collision, the impactor strikes the bumper at a velocity of 4 km/h and moves continuously in the direction perpendicular to the bumper plane. Under the compression of the impactor, the bumper undergoes plastic deformation. In Figure 7, the impactor has already collided with the bumper at 10 ms, resulting in a small deformation of the bumper. As the impactor moves forward, the bumper continues to undergo plastic deformation. By 40 ms, the deformation in the middle part of the bumper is further intensified. At 90 ms, the impactor separates from the bumper. Benefiting from the protective effect and energy absorption capability of the bumper, no significant deformation of the bumper is observed after the separation of the impactor from the bumper.

After analyzing the results of the 100% frontal collision, the contour clouds of stress distribution and deformation distribution of the bumper are obtained, as presented in Figures 8 and 9.

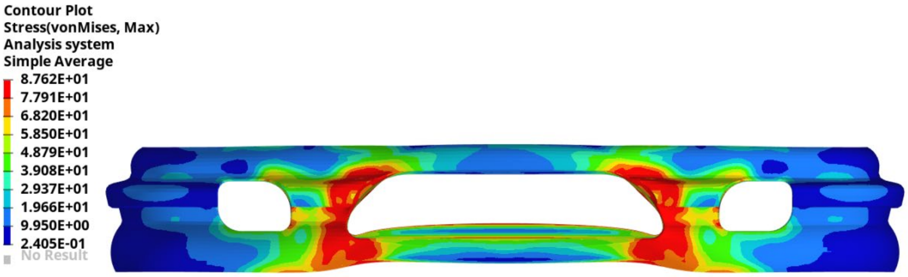


Fig. 8 Contour Cloud of Maximum Stress

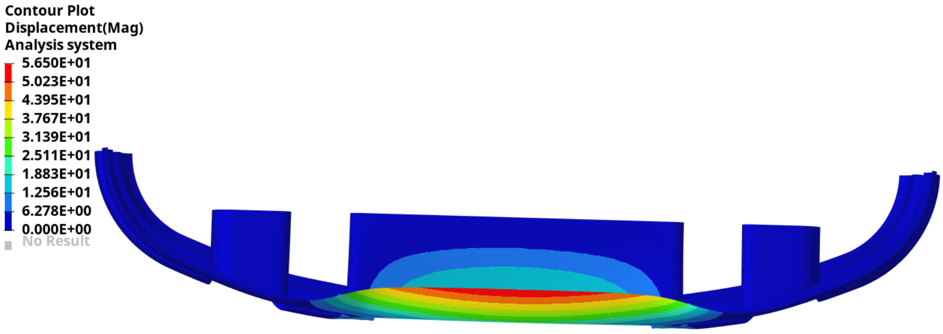


Fig. 9 Deformation Contour Cloud of the Bumper

As observed in Figure 8, the maximum stress of the bumper is 87.6 MPa, which is mainly concentrated in the middle part of the bumper. This is consistent with the results of actual collision tests, and the simulation results are relatively close to the real-world conditions. From Figure 9, it can be seen that the maximum deformation of the bumper is 56.5 mm, which is lower than the designed ultimate tolerance of 68 mm. Meanwhile, during the collision, the anti-collision structures on both sides undergo a certain degree of plastic deformation, indicating that the bumper not only has a certain buffering effect on the collision impact force but also can absorb part of the energy released by the collision.

The displacement-time curve of the impactor is shown in Figure 10. As the impactor moves, it begins to collide with the bumper at 7 ms. The impactor continuously compresses the bumper, and the intrusion depth increases gradually. At 40 ms, the intrusion depth of the impactor reaches its peak; at this moment, the bumper exhibits the maximum deformation of 30.5 mm, and the velocity of the impactor is consistent with the bumper. Subsequently, due to the rebound of the bumper, the intrusion depth decreases gradually. When the collision process ends, the final intrusion depth of the impactor is approximately 8.9 mm.

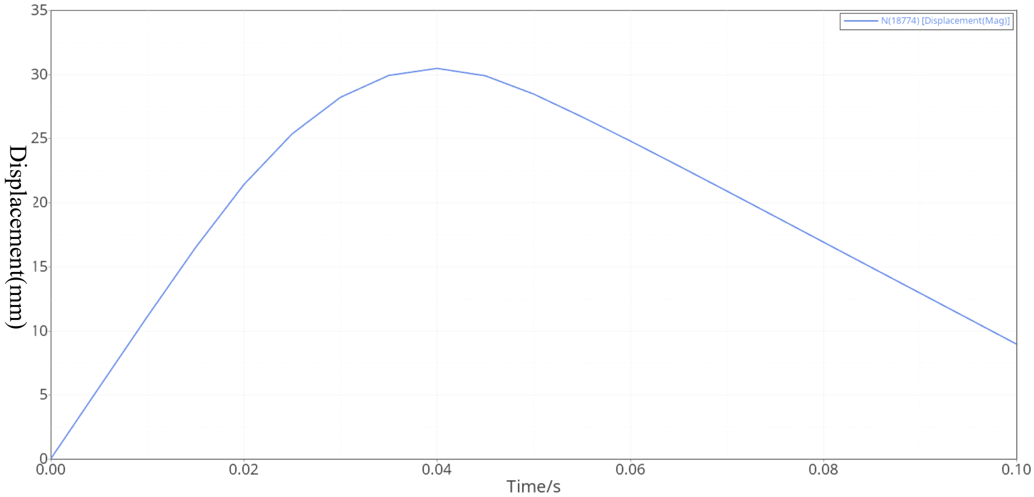


Fig. 10 Diagram of Impactor Intrusion Depth Variation

The analysis results indicate that the designed bumper can effectively absorb the energy generated during the collision process.

### *3.3* **Comparison** ***of Collision Results Under Three Working Conditions***

Using the same parameter settings, the simulation results for the frontal offset collision and 60° angled collision were obtained, with the key result parameters presented in Table 2.

In the 100% frontal collision, the maximum intrusion depth of the anti-collision beam is 30.5 mm, the peak collision force is 56.1 kN, and the maximum energy absorption of the bumper is 68.92 J.

In the offset collision, the maximum intrusion depth is lower than that in the frontal centered collision; the peak collision force, at 42.9 kN, falls between the values of the frontal centered collision and the angled collision; and the maximum energy absorption of the bumper is 71.0 J.

In the 60° angled collision, the maximum intrusion depth of the anti-collision beam is the largest among the three conditions, while the maximum energy absorption of the bumper is the smallest.

Table 2

**Comparison of Indicators for the Three Collision Models**

| Working conditions | Maximum intrusion depth（mm） | Maximum collision force(kN) | Maximum energy absorption(J) |
|---|---|---|---|
| 100% Front-al Collision | 30.5 | 56.1 | 68.9 |
| Offset Collision | 30.0 | 42.9 | 71.0 |
| 60° Angled Collision | 36.0 | 30.4 | 35.5 |

It can be concluded from the comparison that the bumper meets the requirements under all three collision conditions and even has a certain safety margin. However, it is still necessary to conduct reasonable optimization design on the bumper structure.

## 4. Improvement and Optimization Design of the Bumper Structure

There are numerous factors influencing the collision safety performance of bumpers, among which structural design and material improvement are crucial approaches for optimizing bumper performance at present. By making appropriate modifications to the aforementioned bumper model, the mechanical properties of the bumper can be further enhanced in terms of lightweight design and safety.

### *4.1* **Structural** *Improvement of the Bumper*

The thickness of the bumper has a significant impact on the crashworthiness of the vehicle. The original bumper model adopts a thickness of 3.5 mm. From the simulation results, although it exhibits good deformation resistance and collision energy absorption performance, there is a certain degree of structural redundancy under the working conditions of frontal collision, offset collision, and angled collision. Its energy absorption capacity does not reach the material limit, and excessively high structural stiffness is not conducive to pedestrians obtaining "progressive" cushioning protection when colliding with the vehicle [16-18]. Therefore, an attempt was made to reduce the bumper thickness to 2.5 mm, and the same analysis method was used to conduct low-speed collision simulation and optimization analysis. The stress cloud diagram of the bumper under 100% frontal collision obtained from the analysis is shown in Figure 11.

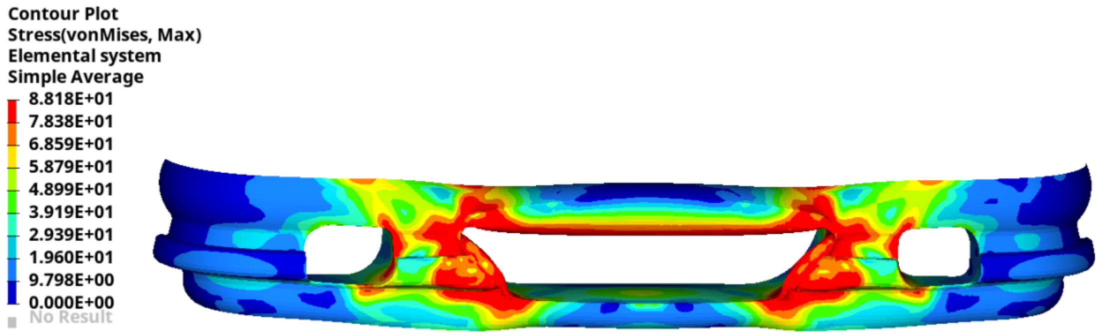


Fig. 11 Contour Cloud of Maximum Stress

As observed in Figure 11, at the moment when the bumper reaches its maximum deformation, the maximum stress borne by the component reaches 88.2 MPa, which is mainly concentrated in the middle area of the bumper. Compared with the state before the thickness adjustment, the maximum stress of the bumper does not change significantly. This indicates that the bumper can still be deformed

Meanwhile, the same simulation analysis was conducted for the three collision conditions, and the obtained collision performance indicators are presented in Table 3.

Table 3

**Collision Analysis Results**

| Working conditions | Maximum intrusion depth (mm) | Maximum collision force(kN) | Maximum energy absorption(J) |
|---|---|---|---|
| 100%Frontal Collision | 48.3 | 30.9 | 69.1 |
| Offset Collision | 58.9 | 30.6 | 69.3 |
| 60° Angled Collision | 61.1 | 25.4 | 34.2 |

In Table 3, under the three collision conditions, the maximum intrusion depth is 61.1 mm (in the 60° angled collision), the maximum peak collision force is 30.9 kN (in the frontal collision), and the maximum energy absorption is 69.3 J (in the offset collision). Compared with the original bumper, it is found that after reducing the thickness, the maximum intrusion depth increases by up to approximately 96.3% (in the offset collision), but it is still far below the limit specified in national standards; at the same time, the peak collision force decreases by 44.9%, which indicates a reduction in the overall structural stiffness and an enhancement in deformability. In addition, the energy absorption ratio per unit mass increases, showing a significant optimization in energy absorption performance, especially in the offset collision, where higher energy absorption reserve is demonstrated.

### *4.2 Material Modification of the Bumper*

The material of the bumper was modified by PP-EPDM-TD20 for better flexibility and impact performance. This material is a composite composed of a PP matrix, supplemented with EPDM modifiers and 20% talc filler. It is widely used in automotive components that require high energy absorption and ductility, such as front grilles, wheel arches, and sill trims. A comparison of material parameters is presented in Table 4.

Table 4 Comparison of Material Properties

| Performance index | PP-LGF30 | PP-EPDM-TD20 |
|---|---|---|
| Density (kg/m³) | 1000 | 980 |
| Elastic Modulus(MPa) | 5600 | 2321 |
| Yield Strength(MPa) | 39.1 | 14.9 |
| Poisson's Ratio | 0.37 | 0.40 |
| Impact Strength (kJ/m²) | Medium to High | Extremely High |

It can be concluded from the comparison that PP-EPDM-TD20 has a lower elastic modulus and yield strength, which enables it to enter plastic deformation earlier during a collision and significantly improve the energy absorption rate. Meanwhile, the presence of EPDM endows the material with excellent low-temperature impact resistance, meeting the requirements for collision performance stability under various climatic conditions. Therefore, on the basis of keeping the bumper structure thickness at 3.5 mm, this study replaced the original material with PP-EPDM-TD20 and conducted low-speed collision simulation analysis.

Under the same numerical simulation settings, the stress distribution of the bumper under 100% frontal collision was obtained, as shown in Figure 12.

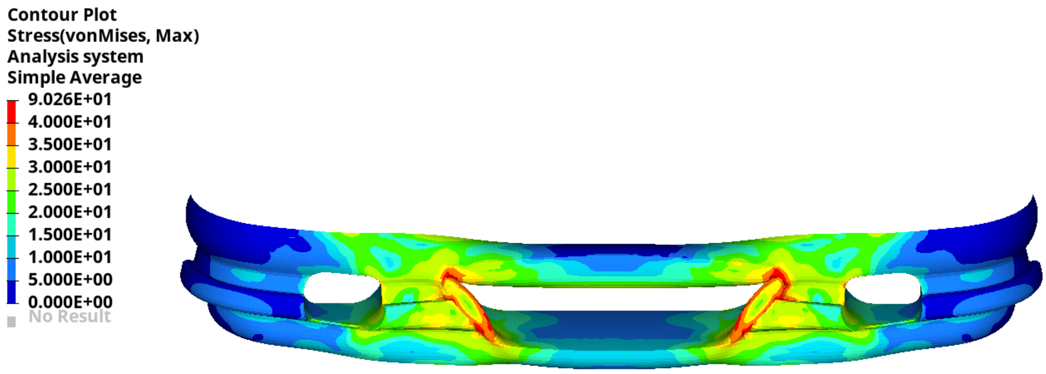


Fig. 12 Contour Cloud of Maximum Stress

As can be seen from Figure 12, at the moment when the bumper undergoes maximum deformation, the maximum stress borne by the component reaches 90.2 MPa, enabling it to fail earlier and absorb collision energy. This meets the collision safety protection performance requirements.

Meanwhile, the same simulation analysis was conducted for the three collision conditions, and the obtained collision performance indicators are presented in Table 5.

Table 5 Comparison Table of Collision Indicators

| Working conditions | Maximum intrusion depth(mm) | Maximum collision force(kN) | Maximum energy absorption(J) |
|---|---|---|---|
| 100%Front-al Collision | 50.4 | 24.3 | 71.7 |
| Offset Collision | 61.3 | 25.0 | 72.1 |
| 60° Angled Collision | 65.5 | 14.2 | 35.8 |

As can be seen from Table 5, under the three collision conditions, the maximum intrusion depth is 65.5 mm (in the 60° angled collision), the maximum peak collision force is 25 kN (in the offset collision), and the maximum energy absorption is 72.1 J (in the offset collision). It can be observed from the comparison that although the intrusion depth increases slightly, it is still far below the standard limit; at the same time, the peak collision force decreases by as much as 56.7% (in the frontal collision), which indicates that the bumper's impact buffering capacity for pedestrians is significantly improved. The maximum energy absorption increases by approximately 4.1%, and the energy absorption ratio per unit mass is significantly optimized. Therefore, PP-EPDM-TD20 material, as a bumper material, not only has excellent collision energy absorption capacity, but also significantly improves the protection effect for pedestrians, and has good engineering adaptability and application promotion value.

In conclusion, whether the thickness of the bumper is reduced to 2.5 mm or its material is replaced with PP-EPDM-TD20, the maximum stress value of the bumper is increased. This enables the bumper to fracture/fail earlier during the collision to absorb collision energy, thereby achieving the protective performance for the vehicle.

## 5. Conclusions

(1) Combined with the national standard GB/T 17354-2024, this paper establishes a low-speed collision FEA (Finite Element Analysis) model for the bumper, and conducts a comparative study on three collision scenarios of the bumper under low-speed conditions: 100% frontal collision, offset collision, and 60° angular collision. By comparing parameters such as impactor intrusion, collision force, and specific energy absorption (SEA) across the three collision conditions, it is found that the 60° angular collision is a relatively severe collision scenario, which should be given sufficient attention in the structural design of the bumper.

(2) Based on the simulation results, the energy absorption characteristics of the bumper are optimized. In terms of structural thickness, the bumper

thickness is optimized from the original 3.5 mm to 2.5 mm. Compared with the previous results, the maximum intrusion increases by approximately 36.9%, and the peak collision force decreases by 44.9%. This indicates that although the overall stiffness of the bumper is reduced and its deformability is enhanced, the energy absorption ratio per unit mass increases, resulting in more prominent energy absorption performance. This is particularly evident under the offset collision condition, where the bumper exhibits higher energy absorption characteristics.

(3) Based on the simulation results, the PP-LGF30 material is replaced with PP-EPDM-TD20. Compared with the previous results, the simulation shows a slight increase in intrusion, a significant decrease of up to 56.7% in the peak collision force, and a 4.1% increase in the maximum energy absorption. These results demonstrate that using PP-EPDM-TD20 as the bumper material can not only improve the energy absorption characteristics of the bumper but also provide better protection for pedestrians.

## REFERENCES

[1] Security Traffic Management of Public. Traffic Management Research Institute of the Ministry of Public Security. Statistical Yearbook on Road Traffic Accidents of the People's Republic of China. 2023.

[2] National Standard of the People's Republic of China. GB 17354-2024: Front and Rear End Protection Devices for Motor Vehicles. 2024

[3] *Nasution Ahmad Yunus, Rejab Mohd Ruzaimi Mat, Ma Quanjin, et al.* Design optimization of passenger SUV's crash box and bumper beam by using finite element method. IOP Conference Series: Materials Science and Engineering, Vol. **1**, Iss. 1068, 2021, 12023.

[4] *Zhengxian Li, Fei Cheng, Yi lin Chen, et al*. Study on Resistance Spot Welding Performance of Al-Si Coated Press Hardening Steels with High Toughness. Automotive Engineering,Vol. **2**, Iss. 47, 2025, pp 367-375.

[5] *Yinghua Yu, Li peng Dong, Ping Xu, et al.*. Discrete element simulation and experimental study on milling force of foam aluminum. Journal of Liaoning Technical University (Natural Science Edition), Vol. **5**, Iss. 42, 2025, pp 601-608.

[6] *Jain Nidhish, Shim Jongmin*. Numerical study on the phononic band-structure of soft granular crystals. International Journal of Solids and Structures, Vol. **191-192**, 2020, pp 173-186.

[7] *Baykasoğlu Adil, Baykasoğlu Cengiz, Cetin Erhan*. Multi-objective crashworthiness optimization of lattice structure filled thin-walled tubes. Thin-Walled Structures, Iss. 149, 2020, 106630.

[8] *Hao Jin, Yu Xiang, Hong hua Jiang, et al.* Multi-objective Optimization of Side Door Bumper Beam for a Passenger Car based on Response Surface Method. Mechanical Science and Technology for Aerospace Engineering, Vol **6**, Iss. 36, 2017, pp 943-949.

[9] J*unjie Wang, Chao Guo, Shou*xin *Li, et al.* Simulation of wave beam barrier collisions and orthogonal test modifications[J]. International Journal of Mechatronics and Applied Mechanics, Vol.**1**, Iss. 18, 2024, pp 84-189.

[10] *Keval Sushruth, Rayapureddi Rakesh, Gurajala Jaswant, et al*. Revamping the vehicle protection system using next-generation car bumper to mitigate pedestrian fatality. International Journal of Crashworthiness, Vol. **6,** Iss. 27, 2022, pp 1770-1789.

[11] *Gonçalves Margarida, Monteiro Helena, Iten Muriel*. Life Cycle Assessment studies on lightweight materials for automotive applications - An overview. Energy Reports, Vol.**8**, 2022, pp 338-345.
[12] Z*hang Shuo, Wang Zhenxing, Zhang Qiang*. Collision simulation and performance improvement evaluation of road guardrails by FEA. International Journal of Mechatronics and Applied Mechanics, Vol.**1**, Iss. 20, 2025, pp 305-310.
[13] *Liu Shi.* Study on Crashworthiness of Automotive Front Anti-Collision Beam under Low-Speed Impact and Multi-Objective Optimization Design. M.A. Thesis, Liaoning Technical University. 2024.
[14] *Xue jing Dou, Zhan li Chen*. Simulation and optimization of frontal collision of the RCAR low-speed structure for pure electric SUV. Journal of Machine Design, Vol. **11**, Iss. 37, 2020, pp 33-41.
[15] *Kaur Rajneet, Singla Sunidhi, Saini N. S.* Head-on collision of nonlinear excitations in electron beam super-thermal plasma. The European physical journal. D, Atomic, molecular, and optical physics, Vol. **8**, Iss. 77, 2023, 162.
[16] *Hui Xie, Ze hao Tang, Hangyan Wang, et al.* Lightweight Research of Bumper Based on Crashworthiness, Journal of Plasticity Engineering, Vol. **3**, Iss. 27, 2020, pp 81-87.
[17] *Kukreja J., Nguyen T., Siegmund T., et al.* Crash analysis of a conceptual electric vehicle with a damage tolerant battery pack. Extreme Mechanics Letters, Vol. **9**, 2016, pp 371-378.
[18] *Gutowski Matthew, Palta Emre, Fang Howie.* Crash analysis and evaluation of vehicular impacts on W-beam guardrails placed behind curbs using finite element simulations. Advances in Engineering Software, Iss114, 2017, pp 85-97.